Generic packing motifs in vapor-deposited glasses of organic semiconductors†

Kushal Bagchi, *[a] Ankit Gujral, [a] M. F. Toney [b] and M. D. Ediger [a]

We study the structure of vapor-deposited glasses of five common organic semiconductors as a function of substrate temperature during deposition, using synchrotron X-ray scattering. For deposition at a substrate temperature of $\sim 0.8T_g$ (where T_g is the glass transition temperature), we find a generic tendency towards "face-on" packing in glasses of anisotropic molecules. At higher substrate temperature however this generic behavior breaks down; glasses of rod-shaped molecules exhibit a more pronounced tendency for end-on packing. Our study provides guidelines to create face-on and end-on packing motifs in organic glasses, which can promote efficient charge transport in OLED and OFET devices respectively.

1. Introduction

Vapor-deposited glasses are a novel class of non-equilibrium solids. As compared to liquid-cooled or spin-coated glasses, they can exhibit greater kinetic stability,[1,2] lower enthalpy[3,4] and higher density.[5] These properties indicate that physical vapor-deposited (PVD) glasses can reside much lower in the potential energy landscape[6] than glasses prepared through any other route.[2] Vapor-deposited glasses can exhibit new dielectric processes[7] that are absent in traditional glasses. At temperatures near zero kelvin, the heat capacity of PVD glasses can disobey thermodynamic relations previously believed to be universal to the glassy state.[8] Vapor-deposited glasses therefore provide new insights into fundamental questions about the "ultimate" properties of amorphous materials.[2]

A key feature distinguishing PVD glasses from conventional glasses is their anisotropic molecular packing.[9–11] Unlike their crystalline counterparts, where the packing arrangements are limited to a few polymorphs, the structure of vapor-deposited glasses can be continuously varied, by changing the deposition temperature.[12,13] Controlling anisotropic structure provides a route to optimize the performance of organic semiconductors in OLED (organic light emitting diode) devices.[14–16] Xing[15] *et al.* showed for films of TCTA that a glass with "face-on" packing exhibits superior charge transport in comparison to a glass with isotropic packing. More recent work by Watanabe *et al.*[17] also found a correlation between face-on packing and charge transport in oligopyridine derivatives. Yokoyama[18] *et al.* showed that glasses with horizontal molecular orientation require a lower driving voltage in devices. Finally, It has also been shown that horizontal molecular orientation is favourable for light-outcoupling in devices.[10] Understanding and controlling the structure of vapor-deposited glasses is of both scientific and technological importance.

The anisotropic structure of vapor-deposited molecular glasses has hitherto been characterized predominantly by optical dichroism measurements.[10,13] Dichroism studies provide the average orientation of a transition dipole moment vector. These studies however lack information on the breadth of the orientation distribution in the glass. Moreover, dichroism measurements are insensitive to correlation lengths, intermolecular distances, or crystallinity. X-ray scattering measurements contain information about all the above, while still being sensitive to molecular orientation. A more holistic measure of structure, provided by X-ray scattering, is needed for a deeper and richer understanding of vapor-deposited glasses. In this paper, we compare the bulk structure of vapor-deposited glasses of five organic semiconductors, with grazing incidence wide angle X-ray scattering (GIWAXS). The glasses are deposited across a substrate temperature range of $0.7–1.0T_g$, where T_g is the glass transition temperature. All the studied molecules are routinely used in OLED devices; Alq3 (tris-(8-hydroxyquinoline)aluminum) is an electron transport material,[19] DSA-Ph (1,4-di-[4-(*N*,*N*-diphenyl)amino]styrylbenzene) is a blue light emitter,[20] TPD(*N*,*N*′-bis(3-methylphenyl)-*N*,*N*′-diphenylbenzidine) is a hole-transport material,[21] m-MTDATA (4,4′,4′′-tris[phenyl(*m*-tolyl)-amino]triphenylamine) is used in hole injection layers[21] and TCTA (tris(4-carbazoyl-9-ylphenyl)amine) is a host-material for emitters.[21]

Our study reveals that at lower deposition temperatures, glasses of anisotropic organic semiconductors exhibit a generic tendency towards "face-on" packing, *i.e.*, these systems tend to

[a] *Department of Chemistry, University of Wisconsin-Madison, Madison, Wisconsin 53706, USA. E-mail: kbagchi@wisc.edu*
[b] *Stanford Synchrotron Radiation Lightsource, SLAC National Accelerator Laboratory, Menlo Park, California 94025, USA*

† Electronic supplementary information (ESI) available. See DOI: 10.1039/c9sm01155b

pack with their aromatic rings perpendicular to the surface normal. It has been argued that the face-on packing motif is favourable for charge transport in OLED devices.[14,15] Calculation of an order parameter, S_{GIWAXS}, using the angular distribution of scattered intensity reveals that the tendency for face-on packing is similar in glasses of anisotropic conjugated molecules deposited at $\sim 0.8T_g$. At higher substrate temperatures, however, we find this generality breaks down; there is more variability in the packing of vapor-deposited glasses of different molecules. Our finding is technologically significant as it suggests that so long as an organic semiconductor has an anisotropic shape, only the appropriate substrate temperature needs to be chosen to produce a glass with face-on packing.

2. Experimental methods

2.1 Sample preparation

All glass films were grown by vapor deposition onto a $\langle 100 \rangle$ silicon substrate (with ~ 2 nm of native oxide) at a deposition rate of ~ 0.2 nm s^{-1} in a high vacuum chamber (base pressure: 10^{-6} Torr). The thickness during deposition was monitored in real time using a Quartz crystal microbalance. After deposition, the thickness was determined precisely by *ex situ* VASE (variable angle spectroscopic ellipsometry) measurements. All the films had a thickness of 100–350 nm; previous studies have shown in this range the structure is independent of thickness.[13,22]

2.2 GIWAXS measurements

Grazing incidence wide angle X-ray scattering (GIWAXS) measurements were performed in beamline 11-3 at SSRL (photon energy $\sim$ 12.7 keV). All measurements were made at room temperature and in a helium atmosphere. The sample to detector distance was calibrated by using the scattering of LaB_6. X-ray scattering patterns were collected at an incidence angle of 0.14°, which is above the critical angle for all the films; the scattering therefore is a measure of the bulk structure. Previous studies have established that for amorphous organic films this angle is appropriate for characterization of bulk structure.[23]

A region of reciprocal space where there are no diffraction peaks was chosen for the background subtraction (the exact regions in reciprocal space for the peak and background can be found in the ESI†). Previous studies from our group did not implement a background subtraction leading to a systematic underestimation of the order parameter. (The background subtracted order parameters for TPD reported here are therefore different from previously published values.[23]) After subtracting the background, the order parameter, described mathematically below, is evaluated:

$$S_{GIWAXS} = \frac{1}{2}\left(3\langle \cos^2 \chi \rangle - 1\right) \quad (1)$$

with $\langle \cos^2 \chi \rangle$ evaluated as follows:

$$\langle \cos^2 \chi \rangle = \frac{\int_0^{90} I(\chi)(\cos^2 \chi)(\sin \chi) d\chi}{\int_0^{90} I(\chi)(\sin \chi) d\chi} \quad (2)$$

3. Results

Shown in Fig. 1 are the molecular structures of the systems that have been investigated in this study. The molecules studied have different shapes. We classify the shapes as "disk-like", "spheroidal" or "rod-like". Although describing a molecule's shape as a rod-like, sphere-like or disk-like, is a simplification, it has previously proved successful in understanding the structure of PVD glasses.[10,24] Previous DFT calculations have shown that, similar to a disk, m-MTDATA and TCTA are planar.[24] Published crystal structures and quantum chemical calculations establish that Alq3,[25] DSA-Ph[26] and TPD[27] are all non-planar. While DSA-Ph and TPD, have a clearly identifiable long-axis like a rod, Alq3 has a more compact molecular shape. For the sake of brevity and simplicity, we henceforth refer to these molecular shapes simply as "rod-like, "disk-like" and "spheroidal".

Shown in Fig. 2 are the GIWAXS patterns from vapor-deposited glasses of the studied molecules, deposited at 0.75–$0.8T_g$. Q_z is the scattering vector out of the plane and Q_{xy} is the scattering vector in the plane. The scattered intensity is represented by colour; red represents high scattered intensity while blue represents low intensity. At substrate temperatures of 0.75–$0.8T_g$ glasses of m-MTDATA, TCTA, DSA-Ph and TPD all exhibit an anisotropic scattering feature at ~ 1.4 $Å^{-1}$. In all these glasses, the excess scattered intensity is along Q_z.; we interpret this anisotropic feature at ~ 1.4 $Å^{-1}$ to arise from molecules packed in a face-on manner. In contrast, vapor-deposited glasses of Alq3 do not exhibit face-on packing; the scattering feature at 1.6 $Å^{-1}$ is isotropic. For PVD glasses of anisotropic conjugated molecules deposited at 0.75–$0.8T_g$, the tendency towards face-on packing seems to be a general feature. The GIWAXS pattern also contain information about the length-scale over which structural order propagates. We observe, using the Scherrer equation[28] that for highly face-on glasses prepared between 0.75–$0.8T_g$, the coherence length (evaluated out of the plane or along all directions) is about 2 nm.

At higher substrate temperatures however, packing is more sensitive to the details of molecular shape. Shown in Fig. 3 are GIWAXS patterns from vapor-deposited glasses of disk-shaped m-MTDATA and rod-shaped DSA-Ph deposited at $0.95T_g$ and T_g.

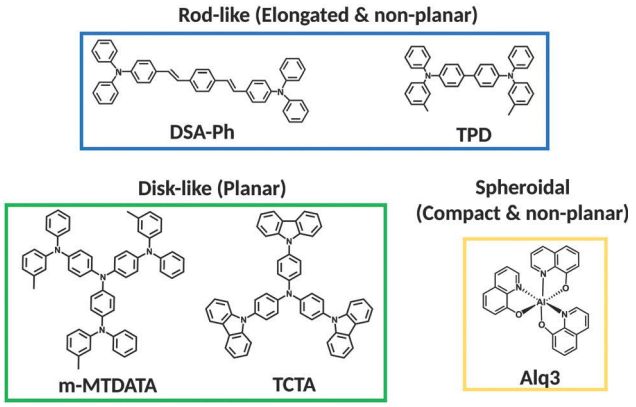

Fig. 1 Molecules used in this study along with their molecular shapes.

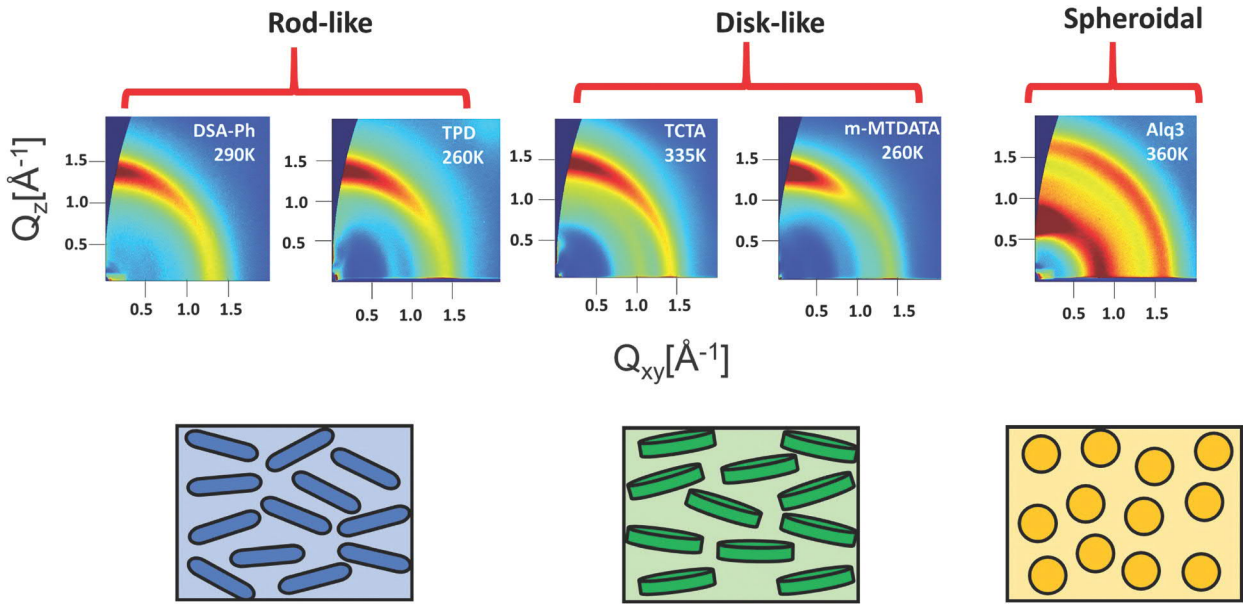

Fig. 2 Grazing incidence X-ray scattering patterns from vapor-deposited glasses of rod-shaped molecules DSA-Ph and TPD, disk-shaped molecules TCTA and m-MTDATA and spheroidal Alq3. All glasses were prepared at $\sim 0.8T_g$, except for m-MTDATA which was prepared at $0.75T_g$. While the peak at ~ 1.4 Å^{-1} is anisotropic for DSA-Ph, TPD, m-MTDATA and TCTA, indicating a tendency for face-on packing, the corresponding peak for Alq3 at 1.65 Å^{-1} is isotropic. The patterns are collected at an incidence angle above the critical angle, therefore probing the bulk structure of the films. Schematic illustrations of the packing arrangements are provided below the scattering patterns.

At $0.95T_g$ we observe that glasses of DSA-Ph clearly exhibit excess scattering intensity along Q_{xy}. This implies that there is an excess population of molecules with end-on packing. In contrast, Fig. 3 shows that PVD glasses of m-MTDATA at $0.95T_g$ exhibit nearly isotropic scattering. Glasses of all the studied molecules prepared at T_g exhibit isotropic scattering; this is expected as glasses prepared at T_g typically exhibit all the same properties as liquid cooled-glasses.[29] Our GIWAXS measurements are consistent with previous dichroism measurements. Walters *et al.* found at $\sim 0.95T_g$ that while there is a pronounced tendency for vertical molecular orientation in glasses of rod-shaped molecules, glasses of disk-shaped molecules exhibit nearly isotropic molecular orientation.[24]

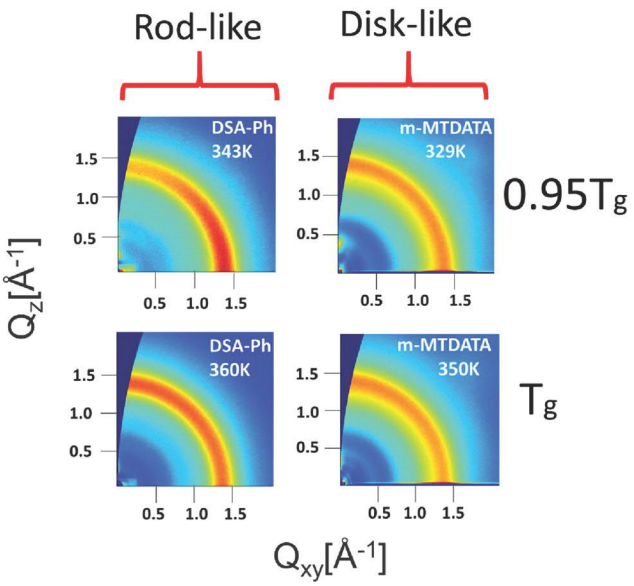

Fig. 3 The grazing incidence X-ray scattering patterns from DSA-Ph and m-MTDATA glasses deposited at $0.95T_g$ and T_g. DSA-Ph exhibits a pronounced tendency for end-on packing when prepared at $0.95T_g$, whereas m-MTDATA prepared at $0.95T_g$ exhibits nearly isotropic scattering. All glasses prepared at T_g exhibit isotropic scattering.

To quantify the scattering anisotropy, we calculate the Herman's order parameter, S_{GIWAXS} for the scattering feature at ~ 1.6 Å^{-1} for Alq3 and ~ 1.4 Å^{-1} for all the other molecules. This feature is sensitive to the π-stacking interactions; the order parameter is therefore loosely a measure of stacking anisotropy. If the order parameter is 1, then all the scattered intensity would be localized along Q_z. This occurs when there is perfect face-on packing. If all the scattering intensity was localized along Q_{xy}, the order parameter would be -0.5. This would occur if there was either perfect end-on or perfect edge-on packing. Calculation of an order parameter requires the scattered intensity as a function of azimuthal angle χ; we define χ to be zero along Q_z and 90° along Q_{xy}. The angular distribution of scattered intensity is evaluated at the peak position for all the glasses.

Shown in Fig. 4 is the Herman's order parameter for glasses of all the studied molecules across a broad range of substrate temperatures. For glasses prepared at substrate temperatures between 0.75–$0.8T_g$, the Herman's order parameter is quite similar for vapor-deposited glasses of DSA-Ph, TCTA and TPD. Of all the molecules, m-MTDATA, exhibits the greatest tendency for face-on packing when deposited at lower substrate temperatures. We speculate that the higher tendency for face-on packing in m-MTDATA glasses prepared at lower temperatures is a combined result of flat molecular shape and a relatively high tendency for horizontal molecular orientation.[24] While glasses of

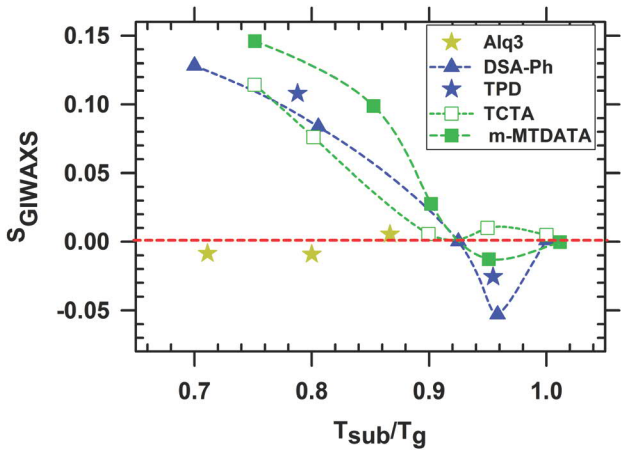

Fig. 4 The S_{GIWAXS} order parameter as a function of substrate temperature plotted for vapor-deposited glasses made from rod-shaped TPD and DSA-Ph, disk-shaped m-MTDATA and TCTA and spheroidal shaped Alq3. The GIWAXS order parameter reported here is a measure of anisotropic structure of the bulk glass. Also note that the Alq3 order parameter characterizes the scattering at $\sim$1.6 Å^{-1}, and not the scattering feature at 0.8 Å^{-1}. The average error in the order parameter, determined from repeating a subset of experiments (both sample preparation and GIWAXS measurement) is $\sim$0.007.

DSA-Ph and TPD can exhibit high tendencies towards horizontal molecular orientation,[13] these molecules are non-planar. TCTA, although flat exhibits a much lower tendency for horizontal molecular orientation[24] when vapor deposited at lower substrate temperatures, as compared to m-MTDATA.[24] Interestingly, the trend in S_{GIWAXS} with substrate temperature for the rod-like and disk-like semiconductors is quite similar for substrate temperatures between 0.75 and $0.9T_g$. In contrast, vapor-deposited glasses of Alq3, do not exhibit face-on packing.

At higher deposition temperatures, both the raw scattering patterns (Fig. 3) and the Herman's order parameter (Fig. 4) indicate that packing is sensitive to the details of molecular shape. Disk-shaped molecules m-MTDATA and TCTA exhibit either negligible or no tendency towards end-on (or edge-on) packing. TPD, a non-planar molecule shows only a small tendency for end-on packing. Glasses of DSA-Ph on the other hand, an elongated rod-shaped molecule shows the strongest tendency for end-on packing. Recent computer simulations of vapor-deposited glasses agree with this observation. Han and co-workers[30] simulated vapor-deposition of four rod-shaped semiconductors; they observed that their longest molecule exhibited the greatest tendency for end-on packing. Consistent with these simulations, we observe that the longer of the two rod-shaped molecules DSA-Ph has the most negative order parameter, S_{GIWAXS}, at $\sim 0.95T_g$, and therefore the greatest tendency for end-on packing. Deposition of even longer molecules at $0.95T_g$ may result in glasses with order comparable to that seen in liquid crystals. This type of end-on packing is desirable for organic field effect transistors.[31]

4. Discussion

Previous studies support our central observation that so long as a molecule is itself anisotropic, it will exhibit face-on packing when vapor-deposited between $0.75–0.8T_g$. Murawski *et al.*[32] vapor-deposited glasses of CBP at room temperature. CBP which has a shape like DSA-Ph and TPD, exhibited face-on packing at room-temperature ($0.77T_g$). The tendency for face-on packing in glasses prepared at lower substrate temperatures is not merely restricted to glasses of small conjugated molecules. At substrate temperatures of $0.75–0.8T_g$, glasses of mesogens triphenylene-ester and phenanthroperylene-ester all exhibit face-on packing.[33] Triphenylene-ester and phenanthroperylene-ester are disk-shaped molecules that have a central planar core with several substituents. Chemical substitutions on the aromatic core and the existence of liquid crystalline states do not change the tendency towards face-on packing in glasses deposited at lower substrate temperature ($0.75–0.8T_g$). It remains unclear whether aromaticity is a pre-requisite for face-on packing. Future X-ray scattering studies on glasses of non-aromatic molecules could answer this question.

Several previous studies have proposed mechanisms to explain the anisotropic structure of vapor-deposited glasses.[4,34,35] These studies attribute the anisotropic structure of a vapor-deposited glass to partial equilibration towards the surface structure of the supercooled liquid. However, recent results on vapor-deposited Posaconazole[36] show that at lower substrate temperatures anisotropic structure is not necessarily an outcome of equilibration towards the surface structure of the equilibrium liquid. In light of these recent results, we speculate that the generic tendency for face-on packing of anisotropic conjugated molecules at lower substrate temperatures is connected to a lack of surface mobility at low temperature. We hypothesize that at lower substrate temperatures, molecules can reconfigure only in a limited manner; these rearrangements being only local in nature. When a molecule lands and attaches to a rigid surface, the easiest way for a molecule to lower its surface energy is by lying flat on the surface. We speculate that the tendency for molecules to lower their surface energy by lying flat gives rise to a tendency for face-on packing at lower substrate temperatures. At higher substrate temperatures ($\sim 0.95T_g$) molecules at the free surface have enough mobility to equilibrate efficiently towards the surface structure of the supercooled liquid. Yu *et al.*[37] have shown that close to T_g, surface diffusion can be seven orders of magnitude higher than bulk diffusion. At higher substrate temperature, due to this high mobility, molecules at the free surface can rearrange collectively towards the macroscopic free energy minimum of the surface. Once the molecules are buried by subsequent deposition they lose their mobility, resulting in surface favoured configurations being trapped into the bulk of the glass. As different molecules have different favoured packing motifs at the free surface, glasses deposited at high substrate temperatures have a range of different structures. The structure of vapor-deposited glasses of Posaconazole supports this hypothesis. Glasses of posaconazole deposited at higher substrate temperature exhibit a strong tendency for end-on packing,[36] consistent with a tendency for end-on packing at the free surface of Posaconazole at equilibrium. At lower substrate temperatures vapor-deposited glasses of Posaconazole exhibit face-on packing, due to limited

surface mobility. Our line of thinking is also consistent with atomistic MD simulations of vapor-deposited CBP glasses performed by Han and co-workers.[30]

Vapor-deposited glasses of Alq3 do not exhibit either face-on or end-on packing, as indicated by the isotropic scattering feature at 1.6 $Å^{-1}$. We attribute this to the more symmetric molecular shape of Alq3, that arises from its chemical bonding. Vapor-deposited glasses of Alq3 however can exhibit a tendency towards ''molecular layering'',[38] as indicated by the anisotropic scattering feature at 0.7 $Å^{-1}$. While the anisotropic scattering intensity arising from face-on packing occurs at a distance close to the π-stacking distance, the layering feature occurs at a distance which is close to the molecular diameter. Glasses of vapor-deposited Ir(ppy)3, a molecule with shape similar to Alq3, exhibit similar scattering patterns. Vapor-deposited glasses of Ir(ppy)3 also exhibit an anisotropic feature associated with layering.[32] Given the similarity in scattering patterns of spheroidal organometallic molecules (like Alq3 and Ir(ppy)3) and the similarity in scattering patterns of more elongated and planar molecules (like m-MTDATA, DSA-Ph, TCTA and TPD), we expect that the scattering pattern of vapor-deposited glasses can be predicted from molecular shape and chemical bonding.

Previous studies have investigated the role of molecular shape in determining the structure of vapor-deposited glasses[10,24] and it is useful to place the present results into this context. Based upon UV-Vis dichroism measurements, Walters *et al.* reported that there is a far greater tendency for horizontal molecular orientation in glasses of rod-shaped molecules than glasses of disk-shaped molecules when deposited at $\sim 0.8T_g$.[24] In contrast, the anisotropic scattering from glasses of rod-shaped and disk-shaped molecules at these substrate temperatures is very similar, as shown in Fig. 4. We can interpret this difference in light of the different information content in these experimental observables. UV-Vis dichroism measurements are sensitive to the orientation of a single axis and thus they cannot distinguish between glasses with face-on and edge-on packing. In contrast, in a GIWAXS pattern, these two packing motifs are easily distinguished. Face-on packing results in excess scattering out of plane (along Q_z at $Q \sim 1.4$ $Å^{-1}$) whereas edge-on packing yields excess scattering in the plane (along Q_{xy} at $Q \sim 1.4$ $Å^{-1}$). In addition to allowing this important distinction, GIWAXS measurements have two additional features important for characterizing vapor-deposited organic semiconductors. Relative to dichroism, GIWAXS is a far more sensitive probe of disorder. For the systems investigated here, the highest GIWAXS order parameter is ∼15% of the theoretical maximum whereas the highest dichroism order parameter for these same systems can reach 80% of the theoretical maximum. In addition, GIWAXS can be used to assess whether the order in the glass is short, medium or long-ranged. The modest coherence lengths that we observe (∼2 nm) even for highly face-on glasses shows that the ordering in vapor-deposited glasses is highly local. These GIWAXS experiments also provide direct evidence that the structural anisotropy in vapor-deposited films is not due to the presence of small crystallites but due to anisotropic glass structure. Thus, in comparison to previous work, GIWAXS provides complementary structural information which allows for a deeper understanding of vapor-deposited materials.

Our study provides a general set of rules for preparing glasses with face-on packing; these rules can be useful for designing organic electronics devices. The packing of a glass is intimately connected to how it transports charge.[39] According to Marcus theory, the rate of charge transport is proportional to the square of the transfer integral; the transfer integral is a measure of how well frontier molecular orbitals on adjacent molecules overlap. Vapor-deposition can produce higher density glasses,[13] which provides one route to increase the transfer integral.[40] Anisotropic packing also increases the transfer integral. For TCTA it has been shown that face-on packing produces a transfer integral roughly twice as large as random packing.[15] More recently it has been shown that increasing face-on packing by engineering weak hydrogen bonds in oligopyridine derivatives can improve charge-carrier mobility. For this case, increasing S_{GIWAXS} by 0.06 was associated with a factor of 6 improvement in electron mobility.[17]

5. Conclusion

We show that the tendency for face-on packing is roughly similar in vapor-deposited glasses of organic semiconductors that (i) have an anisotropic molecular shape and (ii) are prepared at deposition temperature of $0.75–0.8T_g$. Between 0.75 and $0.9T_g$, the trend in the X-ray derived order, as a function of substrate temperature, is also quite similar for four different semiconductors, all of which have an anisotropic molecular shape. Glasses of Alq3, a molecule with a ''spheroidal'' molecular shape do not exhibit face-on packing. At higher substrate temperature there are more variations in the packing of vapor-deposited glasses, as expected given the range of different equilibrium surface structures for organic molecules. The molecule with the most anisotropic shape, DSA-Ph, exhibits the greatest tendency for end-on packing when deposited at $\sim 0.95T_g$. Our study provides general guidelines for preparing glasses with face-on packing and end-on packing. Face-on packing can be used to promote charge transport in OLEDs (organic light emitting diodes) while end-on packing is desirable for OFETs (organic field effect transistors).

Conflicts of interest

There are no conflicts to declare.

Acknowledgements

This work was supported by the US Department of Energy, Office of Basic Energy Sciences, Division of Materials Sciences and Engineering, Award DE-SC0002161. The authors gratefully acknowledge use of facilities and instrumentation supported by NSF through the University of Wisconsin Materials Research Science and Engineering Center (DMR-1720415). Use of the Stanford Synchrotron Radiation Lightsource, SLAC National

Accelerator Laboratory, is supported by the U.S. Department of Energy, Office of Science, Office of Basic Energy Sciences, under Contract DE-AC02-76SF00515.

References

1 C. Rodríguez-Tinoco, M. Gonzalez-Silveira, J. Ràfols-Ribé, A. F. Lopeandía and J. Rodríguez-Viejo, *Phys. Chem. Chem. Phys.*, 2015, **17**, 31195–31201.

2 M. D. Ediger, *J. Chem. Phys.*, 2017, **147**, 210901.

3 S. L. L. M. Ramos, M. Oguni, K. Ishii and H. Nakayama, *J. Phys. Chem. B*, 2011, **115**, 14327–14332.

4 S. L. L. M. Ramos, A. K. Chigira and M. Oguni, *J. Phys. Chem. B*, 2015, **119**, 4076–4083.

5 M. Shibata, Y. Sakai and D. Yokoyama, *J. Mater. Chem. C*, 2015, **3**, 11178–11191.

6 P. G. Debenedetti and F. H. Stillinger, *Nature*, 2001, **410**, 259–267.

7 C. Rodríguez-Tinoco, M. Rams-Baron, J. Rodríguez-Viejo and M. Paluch, *Sci. Rep.*, 2018, **8**, 1380.

8 T. Pérez-Castañeda, C. Rodríguez-Tinoco, J. Rodríguez-Viejo and M. A. Ramos, *Proc. Natl. Acad. Sci. U. S. A.*, 2014, **111**, 11275–11280.

9 H. W. Lin, C. L. Lin, H. H. Chang, Y. T. Lin, C. C. Wu, Y. M. Chen, R. T. Chen, Y. Y. Chien and K. T. Wong, *J. Appl. Phys.*, 2004, **95**, 881–886.

10 D. Yokoyama, *J. Mater. Chem.*, 2011, **21**, 19187.

11 M. D. Ediger, J. J. de Pablo and L. Yu, *Acc. Chem. Res.*, 2019, **52**, 407–414.

12 K. J. Dawson, L. Zhu, L. Yu and M. D. Ediger, *J. Phys. Chem. B*, 2011, **115**, 455–463.

13 S. S. Dalal, D. M. Walters, I. Lyubimov, J. J. de Pablo and M. D. Ediger, *Proc. Natl. Acad. Sci. U. S. A.*, 2015, **112**, 4227–4232.

14 D. Yokoyama, Y. Setoguchi, A. Sakaguchi, M. Suzuki and C. Adachi, *Adv. Funct. Mater.*, 2010, **20**, 386–391.

15 X. Xing, L. Zhong, L. Zhang, Z. Chen, B. Qu, E. Chen and L. Xiao, *J. Phys. Chem. C*, 2013, **117**, 25405–25408.

16 J. Ràfols-Ribé, P. Will, C. Hänisch, M. Gonzalez-Silveira, S. Lenk, J. Rodríguez-Viejo and S. Reineke, *Sci. Adv.*, 2018, **4**, 8332.

17 Y. Watanabe, D. Yokoyama, T. Koganezawa, H. Katagiri, T. Ito, S. Ohisa, T. Chiba, H. Sasabe and J. Kido, *Adv. Mater.*, 2019, **31**, 1808300.

18 J. Y. Kim, D. Yokoyama and C. Adachi, *J. Phys. Chem. C*, 2012, **116**, 8699–8706.

19 C. W. Tang and S. A. VanSlyke, *Appl. Phys. Lett.*, 1987, **51**, 913–915.

20 S. Wen, M. Lee and C. H. Chen, *J. Disp. Technol.*, 2005, **1**, 90–99.

21 Y. Shirota, *J. Mater. Chem.*, 2005, **15**, 75–93.

22 A. Gujral, J. Gómez, J. Jiang, C. Huang, K. A. O'Hara, M. F. Toney, M. L. Chabinyc, L. Yu and M. D. Ediger, *Chem. Mater.*, 2017, **29**, 849–858.

23 A. Gujral, K. A. O'Hara, M. F. Toney, M. L. Chabinyc and M. D. Ediger, *Chem. Mater.*, 2015, **27**, 3341–3348.

24 D. M. Walters, L. Antony, J. J. de Pablo and M. D. Ediger, *J. Phys. Chem. Lett.*, 2017, **8**, 3380–3386.

25 M. Brinkmann, G. Gadret, M. Muccini, C. Taliani, N. Masciocchi and A. Sironi, *J. Am. Chem. Soc.*, 2000, **122**, 5147–5157.

26 M. Ho, C. Chang, T. Chu, T. Chen and C. H. Chen, *Org. Electron.*, 2008, **9**, 101–110.

27 A. R. Kennedy, W. E. Smith, D. R. Tackley, W. I. F. David, K. Shankland, S. J. Teat, I. Facility and C. Rutherford, *J. Mater. Chem.*, 2002, **12**, 168–172.

28 J. Rivnay, S. C. B. Mannsfeld, C. E. Miller, A. Salleo and M. F. Toney, *Chem. Rev.*, 2012, **112**, 5488–5519.

29 S. S. Dalal, Z. Fakhraai and M. D. Ediger, *J. Phys. Chem. B*, 2013, **117**, 15415–15425.

30 Y. Youn, D. Yoo, H. Song, Y. Kang, K. Y. Kim, S. H. Jeon, Y. Cho, K. Chae and S. Han, *J. Mater. Chem. C*, 2018, **6**, 1015–1022.

31 L. Li, W. Hu, H. Fuchs and L. Chi, *Adv. Energy Mater.*, 2011, **1**, 188–193.

32 C. Murawski, C. Elschner, S. Lenk, S. Reineke and M. C. Gather, *Org. Electron.*, 2018, **53**, 198–204.

33 A. Gujral, S. Ruan, M. F. Toney, H. Bock, L. Yu and M. D. Ediger, *Chem. Mater.*, 2017, **29**, 9110–9119.

34 K. L. Kearns, S. F. Swallen, M. D. Ediger, T. Wu, Y. Sun and L. Yu, *J. Phys. Chem. B*, 2008, **112**, 4934–4942.

35 S. Singh and J. J. de Pablo, *J. Chem. Phys.*, 2011, **134**, 194903.

36 J. Gómez, A. Gujral, C. Huang, C. Bishop, L. Yu and M. D. Ediger, *J. Chem. Phys.*, 2017, **146**, 054503.

37 C. W. Brian and L. Yu, *J. Phys. Chem. A*, 2013, **117**, 13303–13309.

38 K. Bagchi, N. E. Jackson, A. Gujral, C. Huang, M. F. Toney, L. Yu, J. J. de Pablo and M. D. Ediger, *J. Phys. Chem. Lett.*, 2018, **10**, 164–170.

39 V. Coropceanu, A. Demetrio, S. Filho, Y. Olivier, R. Silbey and J. Bre, *Chem. Rev.*, 2007, **107**, 926–952.

40 Y. Esaki, T. Komino, T. Matsushima and C. Adachi, *J. Phys. Chem. Lett.*, 2017, **8**, 5891–5897.